Generation of linearized optical single sideband signal for broadband radio over fiber systems

Tao Wang (王 涛), Qingjiang Chang (昌庆江), and Yikai Su (苏翼凯)*

State Key Lab of Advanced Optical Communication Systems and Networks, Department of Electronic Engineering, Shanghai Jiao Tong University, Shanghai 200240

**E-mail: yikaisu@sjtu.edu.cn*

Received June 19, 2008

We propose a new scheme to generate broadband linearized optical single-sideband (OSSB) signal for radio over fiber systems. By using an unbalanced dual parallel Mach-zehnder modulator (DPMZM) followed by optical filtering, a linearized OSSB signal is obtained. With coherent detection, radio frequency (RF) signal can be recovered with simultaneously suppressed second-order distortion and third-order intermodulation. This scheme can be used to realize broadband systems with wide dynamic range.

OCIS codes: 060.0060, 060.2360, 060.5625.
doi: 10.3788/COL20090704.0339.

Radio over fiber (RoF) technique shows advantages including low loss, high bandwidth, and immunity against gelectromagnetic interference. In most RoF systems, input radio frequency (RF) signals are carried on optical carriers via intensity modulation (IM) and recovered after transmission using direct detection (DD) by photodetectors (PDs). Generally, $LiNbO_3$ Mach-Zehnder modulators (MZMs)[1] are utilized for IM/DD links. However, harmonics and intermodulation products are induced due to the sinusoidal transfer characteristic of MZM, which limits the dynamic range of the RoF systems. In addition, a MZM is typically biased at quadrature to low even-order distortion, resulting in a high residual optical-carrier power that may saturate the PD and induce nonlinearity through fiber transmission[2]. Also, the high optical-carrier power increases the intensity noise and shot noise that limit the system dynamic range[3].

To solve the above problems, several techniques have been proposed to mitigate carrier-induced noise and linearize the transfer function of the modulator. Those techniques to suppress optical carrier include optical carrier filtering[4], low biasing of a MZM[5], and class-AB microwave photonics links[6]. Linearization is realized by designing linearized modulators[7,8] and high-linearity PDs[9]. Recently, coherent links are proposed to achieve dynamic range enhancement for better sensitivity[10]. Carrier-suppressed modulation in a coherent system has been demonstrated[11]. However, compared with IM/DD links, higher laser power and lower modulation depth are required to achieve large dynamic range in that scheme.

In this letter, we propose a method to realize large dynamic range by using an unbalanced dual parallel Mach-Zehnder modulator (DPMZM) for linearization. The DPMZM has a structure similar to that used in IM/DD links[12,13]. However, as shown in Fig. 1, the modulator in our scheme is biased at its transmission null and driven by a two-tone RF signal, which generates a suppressed carrier (SC) double-sideband (DSB) signal without high-order components (point A). The signal is then filtered by a following optical bandpass filter (OBPF) to obtain an optical single sideband (OSSB) signal (point B), which can be coherently detected by adding an unmodulated optical carrier (point C) at the transmitter or mixing with an optical carrier provided by local oscillator before beating at the receiver (point D). The second-order terms disappear as the SC modulation is symmetric when the modulator is biased at the null. The third-order intermodulation (IMD3) is reduced by using the linearized DPMZM. In addition, by adjusting the power ratio of the first-order sidebands to the unmodulated optical carrier, a higher fundamental signal power after detection is obtained without increasing the noise floor.

The structure of the proposed DPMZM is shown in Fig. 2. The splitting ratios of the input optical power and the input RF power are 1: γ^2 and 1: α^2, respectively, and the bias conditions are properly chosen. The outputs of two modulators are coherently combined and IMD3 reduction is realized in optical field. The values of α and γ in our scheme are set differently, and it will be proved in the following analysis that they are effective to reduce the IMD3 distortion. Both the primary and secondary modulators are biased at V_π and the phase shift between the two modulators is set to 180°. As a result, a linearized SC-DSB signal can be obtained in optical domain. In order to optimize the values of α and γ for the unbalanced DPMZM, we firstly undertake two-tone analysis. Assuming that the

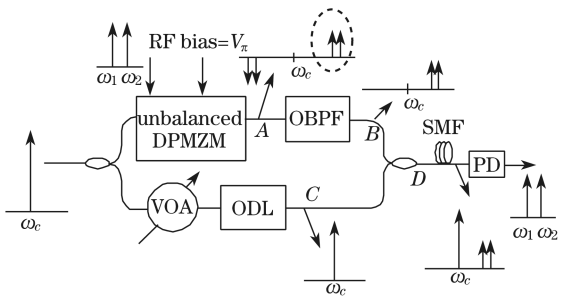

Fig. 1. Schematic of proposed OSSB signal linearization. SMF: single-mole fiber, VOA: variable optical attenuator, ODL: optical delay line.

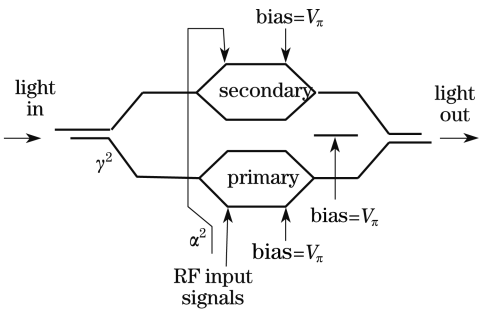

Fig. 2. Structure of unbalanced DPMZM.

two RF tones input to the primary modulator have the same amplitude A and their frequencies are ω_1 and ω_2, respectively, one can get

$$\begin{aligned} V_{\mathrm{in,p}}(t) &= A\sin(\omega_1 t) + A\sin(\omega_2 t), \\ V_{\mathrm{in,s}}(t) &= \alpha V_{\mathrm{in,p}}(t) \end{aligned} \tag{1}$$

where $V_{\mathrm{in,p}}(t)$ is the two-tone RF signal input to the primary modulator and $V_{\mathrm{in,s}}(t)$ is the one into the secondary modulator. For each DPMZM biased at V_π in the unbalanced MZM, if there is a relative 180° difference between the two RF signals, the resulting output optical field can be expressed by

$$\begin{aligned} E_{\mathrm{out}}(t) &= \cos\left\{\frac{\pi}{2V_\pi}[V_{\mathrm{in,p}}(t) - V_\pi]\right\} \mathrm{e}^{\mathrm{j}\frac{\pi}{2V_\pi}V_\pi} E_{\mathrm{in}}(t) - \frac{1}{\gamma}\cos\left\{\frac{\pi}{2V_\pi}[\alpha V_{\mathrm{in,p}}(t) - V_\pi]\right\} \mathrm{e}^{\mathrm{j}\frac{\pi}{2V_\pi}V_\pi} E_{\mathrm{in}}(t) \\ &= \mathrm{j}\left\{\sin\left[\frac{\pi}{2V_\pi}V_{\mathrm{in,p}}(t)\right] - \frac{1}{\gamma}\sin\left[\frac{\pi}{2V_\pi}\alpha V_{\mathrm{in,p}}(t)\right]\right\} E_{\mathrm{in}}(t), \\ E_{\mathrm{in}}(t) &= |E_{\mathrm{in}}|\,\mathrm{e}^{\mathrm{j}\omega_c t}. \end{aligned} \tag{2}$$

Equation (2) can be further expanded by using the Jacobi-Auger expansions, given by

$$\begin{aligned} E_{\mathrm{out}}(t) = \; & |E_{\mathrm{in}}|\left\{\left[J_0(m)J_1(m) - \frac{1}{\gamma}J_0(\alpha m)J_1(\alpha m)\right][\exp(\omega_{\mathrm{c}}+\omega_1)t + \exp(\omega_{\mathrm{c}}+\omega_2)t]\right. \\ & + \left[-J_0(m)J_1(m) + \frac{1}{\gamma}J_0(\alpha m)J_1(\alpha m)\right][\exp(\omega_{\mathrm{c}}-\omega_1)t + \exp(\omega_{\mathrm{c}}-\omega_2)t] \\ & + \left[-J_2(m)J_1(m) + \frac{1}{\gamma}J_2(\alpha m)J_1(\alpha m)\right][\exp(\omega_{\mathrm{c}}+2\omega_2\pm\omega_1)t + \exp(\omega_{\mathrm{c}}+2\omega_1\pm\omega_2)t] \\ & + \left[J_2(m)J_1(m) - \frac{1}{\gamma}J_2(\alpha m)J_1(\alpha m)\right][\exp(\omega_{\mathrm{c}}\pm\omega_2-2\omega_1)t + \exp(\omega_{\mathrm{c}}\pm\omega_1-2\omega_2)t] \\ & + \left[J_0(m)J_3(m) - \frac{1}{\gamma}J_0(\alpha m)J_3(\alpha m)\right][\exp(\omega_{\mathrm{c}}+3\omega_1)t + \exp(\omega_{\mathrm{c}}+3\omega_2)t] \\ & \left. + \left[-J_0(m)J_3(m) + \frac{1}{\gamma}J_0(\alpha m)J_3(\alpha m)\right][\exp(\omega_{\mathrm{c}}-3\omega_1)t + \exp(\omega_{\mathrm{c}}-3\omega_2)t]\right\} \\ & + \text{high order terms}, \end{aligned} \tag{3}$$

where $m = \pi A/2V_\pi$ is defined as the modulation index of the RF signal input to the primary modulator. The optical components we concern about are the first-order terms and the third-order terms because the first-order terms correspond to fundamental signals and the third-order terms generate IMD3 distortion after detection in the receiver. According to the analysis, the coefficients of the terms at the frequencies of $\omega_c \pm \omega_1$ and $\omega_c \pm \omega_2$in Eq. (3) correspond to the normalized amplitudes of the fundamental signals in RF domain, given by

$$x_1 = \left|J_0(m)J_1(m) - \frac{1}{\gamma}J_0(\alpha m)J_1(\alpha m)\right|. \tag{4}$$

The terms at the frequencies of $\omega_{\mathrm{c}}\pm2\omega_{1,2}\pm\omega_{2,1}$ contribute to the third-order distortion in RF domain, given by

$$x_3 = \left|J_2(m)J_1(m) - \frac{1}{\gamma}J_2(\alpha m)J_1(\alpha m)\right|. \tag{5}$$

The terms at the frequencies of $\omega_{\mathrm{c}}\pm3\omega_{1,2}$ are negligible due to their small powers. In order to investigate the optimal values of α and γ, we analyze the relation between the required driving voltage and the output of the fundamental signals to find a balance. We define the optical power penalty (P_{O}) as the ratio of the output optical power of the first-order sidebands generated by the linearized DPMZM to that generated by a conventional push-pull MZM, which is biased at transmission null and driven by the same RF signals. Similarly, an electrical power penalty (P_{E}) is defined as the ratio of the electrical power driving the primary modulator to that driving the secondary modulator. Based on Eq.(3), P_{O} can be obtained as

$$P_{\mathrm{O}} = -20\lg\frac{\left|J_0(m)J_1(m) - \frac{1}{\gamma}J_0(\alpha m)J_1(\alpha m)\right|}{J_0(m)J_1(m)}, \tag{6}$$

and P_{E} can be provided as

$$P_{\mathrm{E}} = 20\lg\alpha. \tag{7}$$

The relation between P_{O} and P_{E} is illustrated in Fig. 3, assuming that the value of m and the relationship

$\alpha^3 = \gamma$ are fixed. It can be seen that $P_{\rm O}$ decreases with the increase of $P_{\rm E}$. Thus, the optimal value of α can be obtained when balancing $P_{\rm O}$ and $P_{\rm E}$. At an optical power penalty of 3 dB, the corresponding electrical power penalty is 4.8 dB, where the tradeoff between $P_{\rm O}$ and $P_{\rm E}$ is obtained. Thus, the corresponding optimal value of α is ∼1.75. In IM/DD links[12], it was proved that there was certain improvement in IMD3 reduction if the value of α and γ were slightly off the exact relation of $\alpha^3 = \gamma$. To set the optimal value of γ, we define the intermodulation to carrier ratio (ICR) as

$$\mathrm{ICR} = 20\lg\left|\frac{J_2(m)J_1(m) - (1/\gamma)J_2(\alpha m)J_1(\alpha m)}{J_0(m)J_1(m) - (1/\gamma)J_0(\alpha m)J_1(\alpha m)}\right|, \quad (8)$$

which describes the ratio of the output field of third-order sidebands to that of the first-order sidebands. The performance of IMD3 reduction is assessed by the value of ICR.

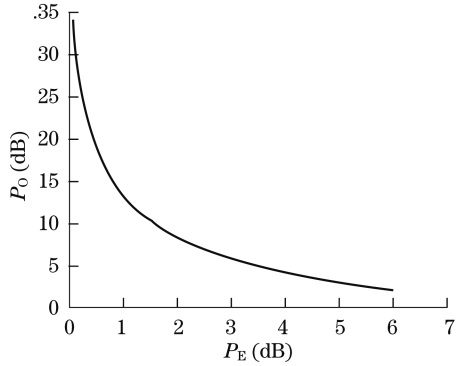

Fig. 3. Relation between electrical and optical power penalties, assuming modulation index m is fixed at 0.3 and $\alpha^3 = \gamma$.

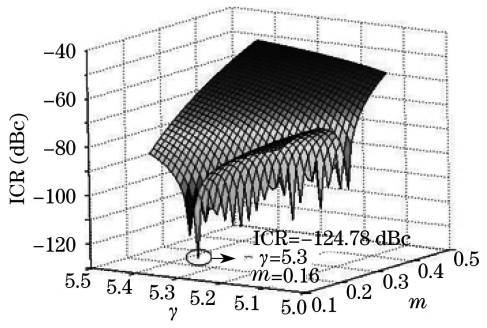

Fig. 4. Functional behavior of ICR for two-tone analysis. γ is optical splitting ratio between primary and secondary modulator, m is modulation index.

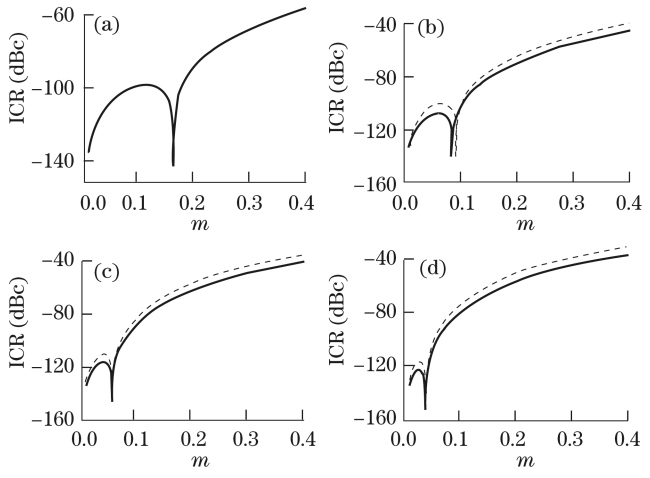

Fig. 5. Calculated ICR varies with the value of modulation index m in different cases. (a) Two-tone RF signal, (b) four-tone RF signal, (c) eight-tone RF signal, (d) sixteen-tone RF signal. Solid line: ICR analysis based on third-order terms at $\omega_{\rm c}\pm2\omega_l\pm(-\omega_m)$; dashed line: ICR analysis based on third-order terms at $\omega_{\rm c}\pm\omega_l\pm\omega_m\pm(-\omega_n)$.

We perform numerical calculations by MATLAB to find the optimal setting of γ in order to achieve the desired performance of IMD3 reduction. Firstly, we set the value of α to 1.75, i.e., the splitting ratio of the electrical power is ∼1:3.0. Figure 4 shows the relation among the values of γ, m, and ICR. It can be seen that the lowest ICR is obtained when the valuse of γ is about 5.3, and with the increase of m, the value of γ increases correspondingly to maintain low ICR. Based on the numerical calculation, the lowest ICR is about −124.78 dBc, which is achieved by setting γ=5.3 and $m = 0.16$. Using these values, IMD3 can be reduced below the noise floor at a given input optical power from laser in the simulations. In that case, the splitting ratio of input optical power is ∼1:28, implying that the designed DPMZM can be fabricated in practice. In the following analysis, we fix the parameters α and γ of the linearized DPMZM (α=1.75 and γ=5.3). We consider the ICR performance with different input RF signals. Figure 5 shows that the ICR varies with the modulation index m in different cases with two-tone, four-tone, eight-tone, and sixteen-tone input RF signals. In the two-tone RF inputsignal case (Fig. 5(a)), it can be seen that ICR increases gradually with the increase of m. However, there is a "dip" appearing at a particular value of m. In the cases of multi-tone RF signals injected to the linearized DPMZM, there is similar characteristic to the two-tone RF signal case. The difference is that additional third-order terms at $\omega_{\rm c} \pm \omega_l \pm \omega_m \mp \omega_n$ are induced in optical domain. Similar to the analysis of two-tone input RF signal based on Jacobi-Auger expansions, we can conclude that the optical field of three-order terms at $\omega_{\rm c} \pm \omega_l \pm \omega_m \mp \omega_n (l \neq m \neq n)$ is proportional to $J_0^{N-3}(m)J_1^3(m) - J_0^{N-3}(\alpha m)J_1^3(\alpha m)/\gamma$, while the optical field of third-order terms at $\omega_{\rm c} \pm 2\omega_i \pm \omega_j (i \neq j)$ is proportional to $J_0^{N-2}(m)J_1(m)J_2(m) - J_0^{N-2}(\alpha m)J_1(\alpha m)J_2(\alpha m)/\gamma$. The optical field of first-order terms is proportional to $J_0^{N-1}(m)J_1(m) - J_0^{N-1}(\alpha m)J_1(\alpha m)/\gamma$, where N is the number of input RF tones ($N > 2$). According to the analysis, ICR can be calculated, as shown in Figs. 5(b)−(d), which correspond to the cases with four-tone, eight-tone, and sixteen-tone RF input signals, respectively. The solid line illustrates the calculated value of ICR, which is the ratio of the optical field of third-order terms at $\omega_{\rm c} \pm 2\omega_l \mp \omega_m$ to that of first-order terms, while the dashed line illustrates another calculated value of ICR, which is the ratio of the third-order terms at $\omega_{\rm c} \pm \omega_l \pm \omega_m \mp \omega_n$ to that of first-order terms. As shown in Fig. 5, the value of m, corresponding to the low ICR value (< 80 dBc), decreases with the number of input RF tones increasing. In other words, with the

increasing number of input RF tones, the input powers have to decrease correspondingly for achieving low ICR. For two-tone, four-tone, eight-tone, and sixteen-tone RF signals, the optimal modulation indices are about 0.16, 0.08, 0.06, and 0.04, respectively. Thus, the powers of output RF fundamental signals decrease with the number of input RF tones increasing.

To better illustrate our scheme, we consider transmitting two RF tones at $f_1 = 9$ GHz and $f_2 = 10$ GHz by simulations. A continuous-wave (CW) laser is set to 1550 nm with a linewidth of 10 MHz. In order to achieve $m = 0.16$ under the condition that the RF power split ratio is fixed at 1: 1.75^2, the amplitude of the two-tone RF signal input to the primary MZM is 0.4 V and that the input to the secondary MZM is 0.7 V, respectively, assuming that V_π of the primary and secondary modulators is 4 V. The modulated OSSB signals are detected in the PD with a responsivity of 1.0 A/W and a thermal noise of $10^{-12}\mathrm{A}/\sqrt{\mathrm{Hz}}$. The shot noise is also considered. Simulations are carried out with the software VPI TransmissionMaker.

Figure 6 shows the simulated optical spectrum at the output of the linearized DPMZM. It is shown that there are only first-order components at $\omega_c \pm \omega_1$ and the second-order and third-order components are significantly suppressed. After passing through the filter, only the lower sidebands are combined with the unmodulated optical carrier to generate the OSSB+C signal, as shown in Fig. 7(a).

We first consider a B-to-B system. Figure 8 shows a comparison of the simulated RF fundamental signals and IMD3 power using the proposed linearized OSSB-signal generation scheme and the conventional method. The input optical powers from the laser are set equal in two schemes. One can see from Fig. 8(a) that the nonlinear distortion power is suppressed under the noise floor due to the linearization process. However, after transmission over 25 km of single-mode fiber (SMF) with an attenuation of 0.2 dB/km and a chromatic dispersion of 16 ps/(nm·km), the output noise in electrical domain increases while the power of fundamental signals decreases, as shown in Fig. 9(a). Thus the output signal-to-noise ratio (SNR) decreases and the performance of the system is degraded. Through injecting more optical power into the linearized DPMZM with less optical power for the optical carrier by using unequally split coupler, e.g., 95:5 coupler, the modulation depth can be increased significantly, as shown in Fig. 7(b). In Fig. 9(b), the noise power is

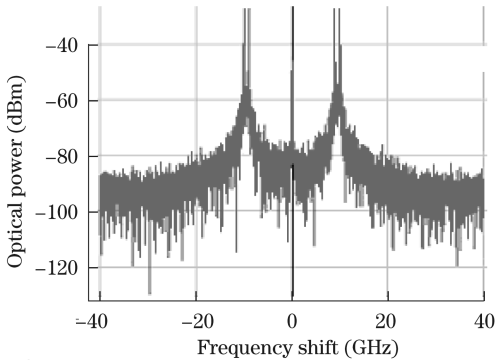

Fig. 6. Simulated optical spectrum of the output of the unbalanced DPMZM. The center frequency is 193.1 THz.

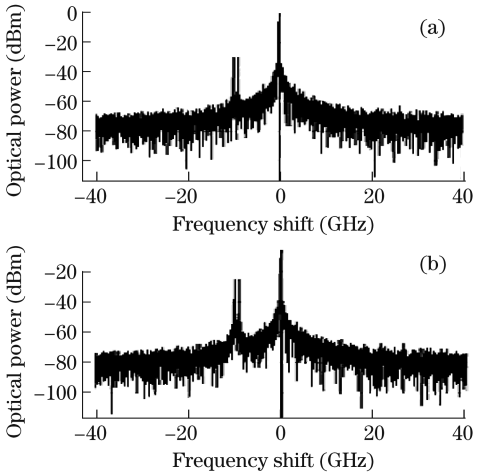

Fig. 7. Simulated optical spectra of the output OSSB+C signal (a) without and (b) with enhanced power ratio of first-order sidebands to optical carrier.

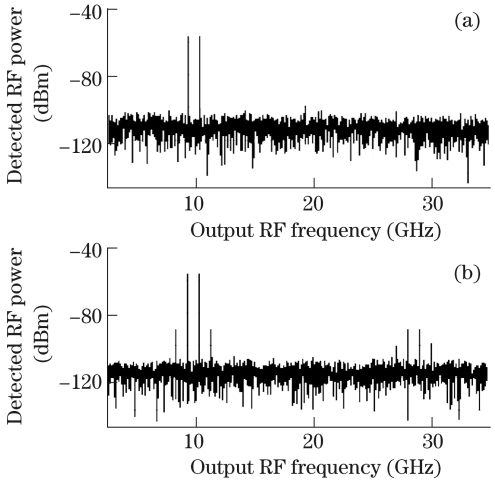

Fig. 8. Simulated RF spectra after detection using (a) our linearization scheme and (b) the conventional method in a B-to-B configuration.

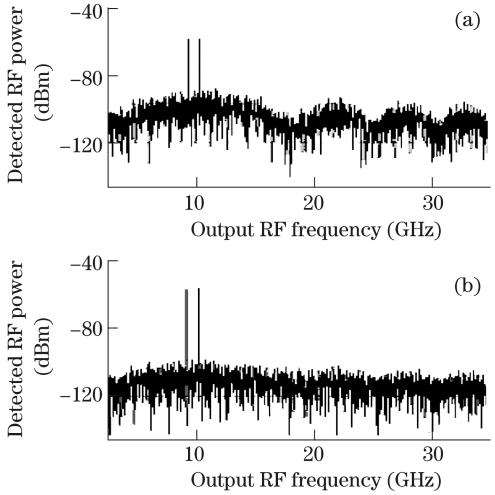

Fig. 9. Simulated RF spectra (a) without and (b) with enhanced power ratio of first-order sidebands to optical carrier after transmission over 25-km SMF.

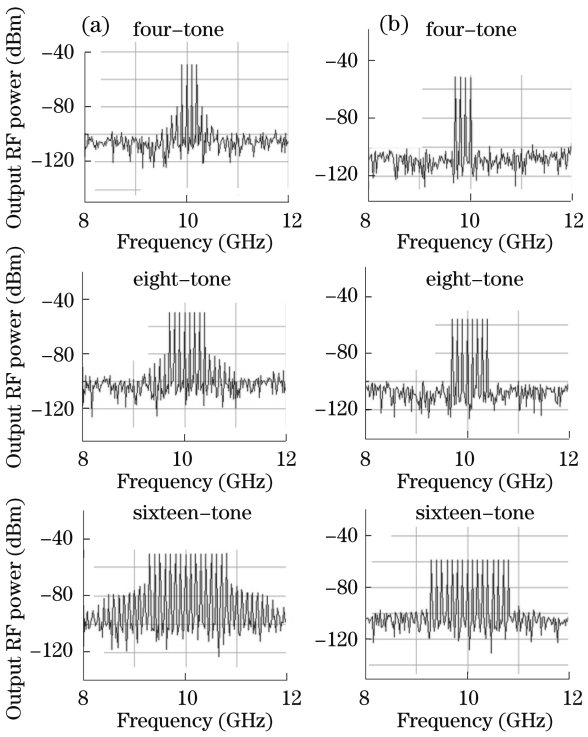

Fig. 10. Optical spectra of multi-tone SC-DSB modulated signals (a) without and (b) with linearization.

effectively reduced by using this method. The optimal state is that the power of the sidebands is approximately equal to that of the optical carrier. We also perform simulations for four-tone, eight-tone, and sixteen-tone RF signals, respectively. By setting the optimal value of m, IMD3 can be significantly reduced under the noise floor, as shown in Fig. 10.

In conclusion, we have proposed and investigated a linearization scheme to reduce the IMD3 for OSSB signal. An unbalanced DPMZM is designed and it is proved to be an effective way to realize IMD3 reduction. Two-tone RF signal analysis and simulations show that ICR can achieve up to −124.78 dBc, implying that the IMD3 can be suppressed under the noise floor. In addition, simulation results prove that ICR improvement can also be achieved for multi-tone RF signals. Thus, the linearized OSSB signal can be applied to the broadband analog transmission systems.

This work was supported by the National "863" Project of China under Grant No. 2006AA01Z255.

References

1. J. Lu, W. Wang, Y. Li, X. Zheng, and H. Zhang, Acta Opt. Sin. (in Chinese) **27,** 159 (2007).
2. K. J. Williams, R. D. Esman, and M. Dagenais, J. Lightwave Technol. **14,** 84 (1996).
3. M. L. Farwell, W. S. C. Chang, and D. R. Huber, IEEE Photon. Technol. Lett. **5,** 779 (1993).
4. R. D. Esman and K. J. Williams, IEEE Photon. Technol. Lett. **7,** 218 (1995).
5. L. T. Nichols, K. J. Williams, and R. D. Esman, IEEE Trans. Microwave Theory Tech. **45,** 1384 (1997).
6. J. D. Bull, T. E. Darcie, J. Zhang, H. Kato, and N. A. F. Jaeger, IEEE Photon. Technol. Lett. **18,** 1073 (2006).
7. B. Masella and X. Zhang, IEEE Photon. Technol. Lett. **19,** 2024 (2007).
8. T. Kishino, R. F. Tavlykaev, and R. V. Ramaswamy, IEEE Photon. Technol. Lett. **12,** 1474 (2000).
9. J. Klamkin, A. Ramaswamy, L. A. Johansson, H. -F. Chou, M. N. Sysak, J. W. Raring, N. Parthasarathy, S. P. DenBaars, J. E. Bowers, and L. A. Coldren, IEEE Photon. Technol. Lett. **19,** 149 (2007).
10. Y. Li, D. Yoo, P. Herczfeld, A. Rosen, A. Madjar, and S. Goldwasser, in *Proceedings of International Topical Meeting on Microwave Photonics* 273 (2005).
11. G. E. Betts, in *Proceedings of LEOS 2004* MN3 (2004).
12. S. K. Korotky and R. M. De Ridder, IEEE J. Sel. Areas Commun. **8,** 1377 (1990).
13. J. L. Brooks, G. S. Maurer, and R. A. Becker, J. Lightwave Technol. **11,** 34 (1993).